J Electroceram (2009) 23:262–271
DOI 10.1007/s10832-008-9418-1

Operating frequency tracking of single phase driving type piezoelectric motors

Burhanettin Koc

Received: 1 June 2007 / Accepted: 8 January 2008 / Published online: 29 January 2008

Abstract We developed a multi (or mixed) mode excitation type piezoelectric motor that uses a rectangular bar type piezoelectric multilayer stator as the vibrating element. The stator has a first longitudinal vibration mode in a direction of longest length and second flexural mode in a direction of thickness. During operation of the motor, these two modes are coupled so at the two end surfaces, elliptical motions are generated. The elliptical motion at one end of the stator is transferred to a moving element through frictional contact. This paper introduces structure and operating principal of the piezoelectric multilayer stator. An equivalent circuitry model for the free stator and a frequency tracking method to operate the motor at its optimum operating frequency are also proposed. The frequency tracking method not only finds the best operating frequency, it also tracks the frequency variations from sample to sample and operating frequency shift due to temperature change.

Keywords Piezoelectric · Multilayer · Multi-mode · Motor · Equivalent circuitry · Frequency tracking

1 Introduction

In many portable devises, a mechanical positioning in a small volume is needed for various reasons. One example of such a need is positioning of a lens group in a camera module of a mobile phone for optical zooming or focusing applications. Due to requirement of a gearbox, traditional electromagnetic solutions for lens moving mechanism can not fulfill the demand. In addition, they have power consumption limitations. On the other hand, piezoelectric motors with their exceptional properties like direct drive and a holding torque without a gearbox or a brake mechanism are a promising solution for aforementioned application.

In literature, many different types of piezoelectric motor structures exist with a common principal that is; small vibratory motion is transferred to the slider or moving element through frictional contact between vibrating and sliding body. Exciting at least two orthogonal resonance modes of the vibrating body generates elliptical motion on the stator surface. Among various types of piezoelectric ultrasonic motors [1–8] such as traveling wave, standing wave, smooth impact drive and multi mode excitation types, multi mode excitation type piezoelectric motors have advantages of single phase driving and less number of components [9, 10].

Principal of multi (or mixed) mode excitation type piezoelectric motor using rectangular type bulk piezoelectric elements was proposed in 1976 [11, 12]. The vibrator is a piezoelectric plate with four segmented electrode on front surface and uniform electrode on the back surface. Segmented electrodes are excited simultaneously so that two orthogonal modes that are first longitudinal and second flexural in width direction are excited at the same time causing side surface points make elliptical motions. These elliptical motions are transferred to a slider that is touching to the vibrating body with a force applied by a pre-stress spring.

The piezoelectric motor that we are introducing in the following section is also a multi mode excitation type. After introducing operating principal of the motor, we will describe piezoelectric multilayer stator manufacturing tech-

B. Koc (✉)
Samsung Electro-Mechanics Co., Ltd.,
Suwon 443-743, South Korea
e-mail: b.koc@samsung.com

niques and internal electrode connectivity of the stator. Simplified equivalent circuitry of the free stator and single phase driving with operating frequency tracking method will be described before concluding the paper.

2 Structure of the stator

As a principal, in single phase multi mode excitation type piezoelectric motors, the vibrating stator element has two channels with a common ground. When one channel in these motors is driven, only half volume of the vibrating body is electrically excited. Even if half of the piezoelectric volume is excited, whole stator body with attached additional elastic elements, such as friction layer, vibrates.

The motor that we are introducing hereafter has three layers of piezoelectric ceramic plates. As shown in Fig. 1, top electrode are divided by two sections to form channel 1 (Ch1) and channel 2 (Ch2). Bottom electrode is uniform and mutual ground (GRN) to channels 1 and 2. The corresponding internal electrodes are connected to top and bottom electrodes through two side electrodes and one end electrode.

When, channel 1 is driven with an electrical signal, top left side; middle right and bottom right sides of the piezoelectric ceramic layers are excited. Similarly, when channel 2 is driven, top right side: middle left and bottom left sides of the piezoelectric ceramic layers of the stator are excited. The dimension of the stator is designed so that two orthogonal modes, which are first longitudinal, and second thickness bending mode resonance frequencies to be equal. For either electrical excitation; channel 1 or 2, even if half of the volume is electrically excited, the whole stator vibrates. Since at operating frequency the excited modes are orthogonal, the resulting motion at the end of the stator is in

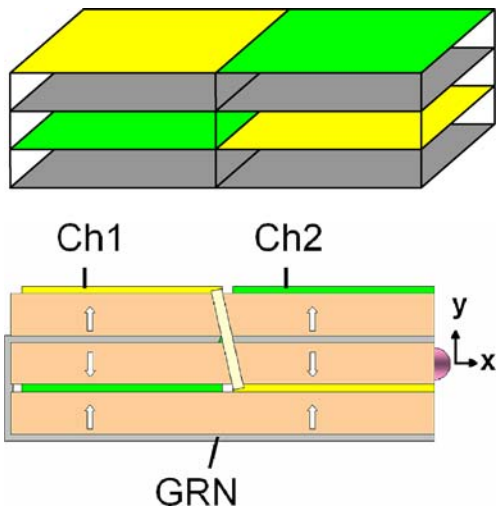

Fig. 1 Surface conductive electrodes (*top*) and cross-sectional view of the stator that has three terminals; Ch1, Ch2 and Ground (*bottom*)

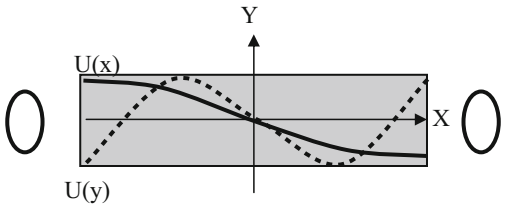

Fig. 2 Displacement in length (*solid line*) and thickness directions (*dashed line*). $U(x)$ is magnitude of displacement in x direction and $U(y)$ is magnitude of displacement in y direction

elliptical form. Exciting channel 1 or 2 is altering the direction of this elliptical motion. Figure 2 shows an example of displacement magnitude of the two orthogonal modes, first longitudinal and second bending in thickness direction.

In order to excite two orthogonal modes, which are first longitudinal and second bending modes, geometry of rectangular stator need to be optimized. Since the stator has a rectangular prism shape, the only variables are length, width and thickness. All the conductive electrodes excluding side electrodes are applied on a surface bounded by width and length, narrowness of width of the stator is defined by manufacturability limits. In principal internal electrode design should not let the structure vibrates in width direction, which would decrease the efficiency. Therefore, width of the stator was not used as design parameter. Length of the stator on the other hand is application specified; it can be defined by space available in actuating system. Thickness of the stator was optimized using ATILA finite element program for various lengths. While the first longitudinal mode is almost independent from the thickness of the stator, dependency of second bending mode is roughly square root of the thickness. These first longitudinal and second bending mode shapes are seen in Fig. 3. As a design parameter, various stator length to optimum thickness as a function of frequency is shown in Fig. 4. The two orthogonal modes are matching at a frequency that length to thickness ratio is constant and this constant number is 3.3.

3 Multilayer stator manufacturing

In order to increase manufacturability and decrease driving voltage of the motor, we manufactured these stators using conventional multilayer actuator manufacturing techniques and for that a special electrode structure was designed [Fig. 5(b)]. A stator array was manufactured at one time using already known co-firing multilayer actuator manufacturing technique, such as tape casting method. Later this stator array was sliced to make each unit cells [Fig. 5(a)]. Figure 6 shows the stators with various dimensions; length

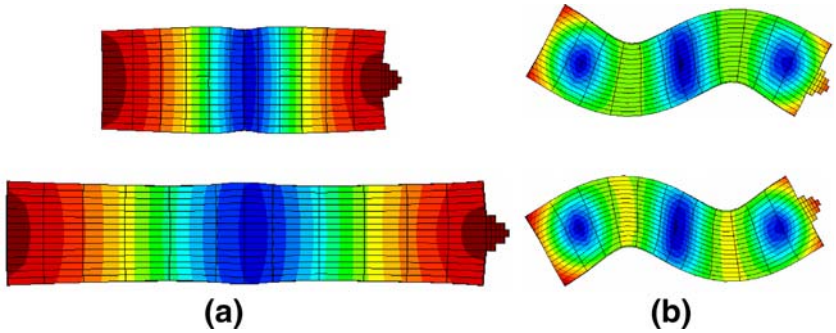

Fig. 3 (**a**) First longitudinal mode shapes in length direction. (**b**) Second flexural mode shapes in thickness direction. In order to excite an elliptical motion at the end of the stator, these two orthogonal modes need to be excited at the same time

ranging from 3.5 to 7.0 mm with corresponding thicknesses that the constant ratio of 3.3 was maintained.

4 Modeling of simplified equivalent circuitry of the free stator

Since the vibrating stator element of the designed motor is single phase mixed mode excitation type, to obtain equivalent circuitry of the free stator, we have treated it as a piezoelectric transformer [13, 14]. Admittance spectra of free stator were measured for six different cases.

Case 1 Ch1 and Ch2 terminals were connected to "HIGH" side and GRN terminal to "LOW" side of the impedance analyzer (HP 4194A). Since this type of driving is equivalent to a resonator, only first longitudinal mode is excited. In this case the DC capacitance value is parallel connection of the channel 1 and channel 2 capacitances [Fig. 7(a)]. The magnitude and phase of the first pure longitudinal mode curves are the thin solid line in Fig. 8(a) and (b) (the cures are labeled as "L1_WO/TIP").

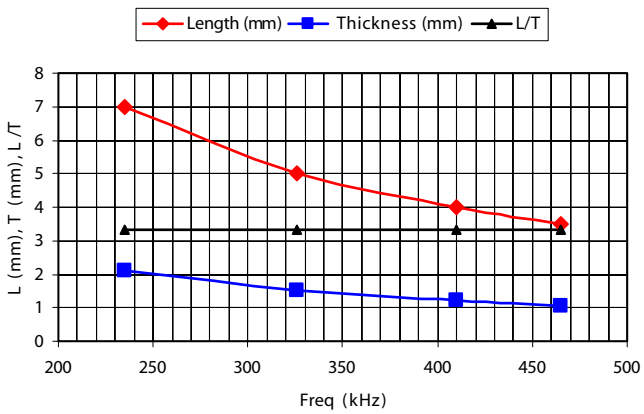

Fig. 4 At matching frequency length to the thickness ratio of the stator is constant and the constant number is 3.3

Case 2 Ch1 terminal was connected to "HIGH" side and Ch2 terminal to "LOW" side of the impedance analyzer. Ground (GRN) terminal was leaved floating. In this case only second bending mode is excited. At off resonance, DC capacitance values are the serial connection of channel 1 and channel 2 capacitances [Fig. 7(b)]. The magnitude and phase of the second pure bending mode curves are the thick solid line in Fig. 8(a) and (b) (the curves are labeled as "B2_WO/TIP").

Case 3 Ch1 terminal was connected to "HIGH" side and GRN terminal was connected to "LOW" side of the impedance analyzer (Ch2 terminal was leaved floating). This case is normal motor operation and both modes are excited even though only one channel is excited. At off resonance, DC capacitance values are the capacitance of only channel 1 [Fig. 7(c)]. The magnitude and phase of the first longitudinal and second bending mode curves are the line with square shaped empty dots in Fig. 8(a) and (b) (the curves are labeled as "L1_B2_WO/TIP"). From the comparison of admittance curves, we can see that anti-resonance frequencies of pure first longitudinal mode for "Case 1" driving and anti-resonance frequency of "Case 3" driving are overlapping for both magnitude and frequency values. Similarly pure second bending mode anti resonance frequency for case 2 driving is equal to second bending mode anti-resonance frequency for case 3 driving.

Case 4 Ch1 terminal was connected to "HIGH" side and GRN terminal was connected to "LOW" side of the impedance analyzer. Ch2 terminal was shorted to GRN terminal. In this case also both first longitudinal and second bending modes are excited. At off resonance, DC capacitance values are the capacitance of only channel 1 [Fig. 7(c)]. The magnitude and phase of the first longitudinal and second bending mode curves are the line with triangle shaped filled dots in Fig. 8(a) and (b) (the

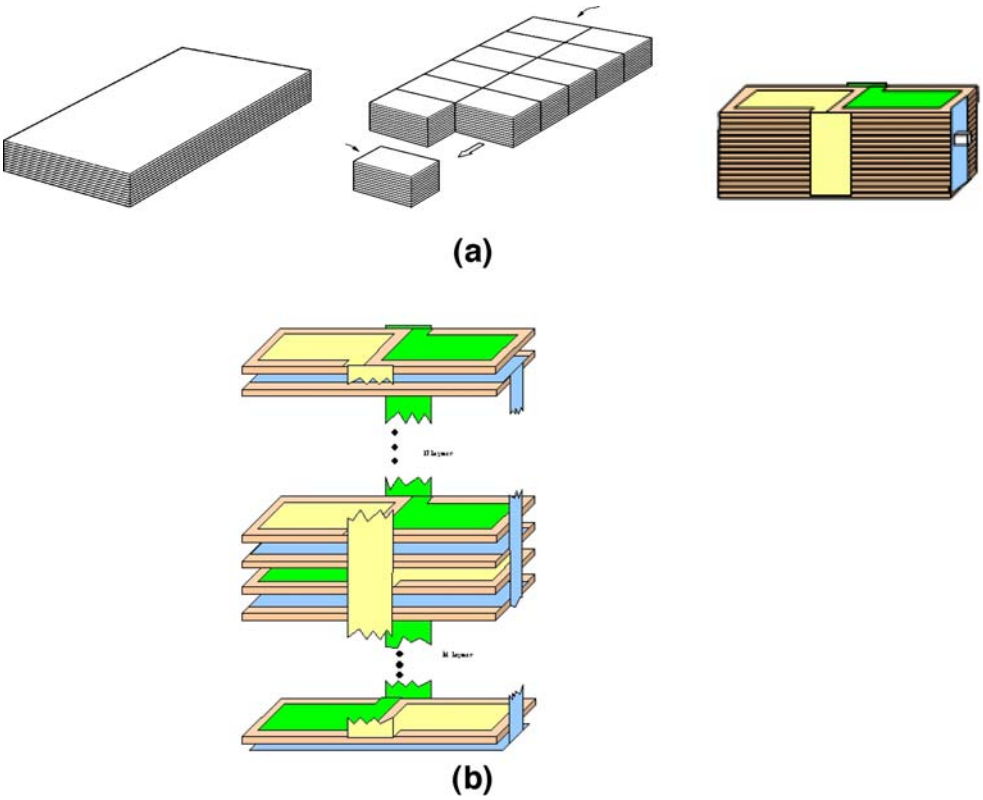

Fig. 5 (**a**) Simplified co-fired multilayer piezoelectric stator manufacturing process, (**b**) stator exploited perspective view showing internal and outside termination electrodes

curves are labeled as "L1_B2_GRN_WO/TIP"). From the comparison of admittance curves, it was observed that resonance frequency of pure second bending mode for cases 2 and 3 driving; both magnitude and frequency values are equal. Similarly for pure first longitudinal mode resonance frequencies for cases 1 and 3 driving are equal.

It was also observed that phase curves of pure bending and pure longitudinal modes of "Case 1" and "Case 2" driving are making an envelope to phase curves of bending and longitudinal modes of "Case 3" and "Case 4" driving [Fig. 8(b)].

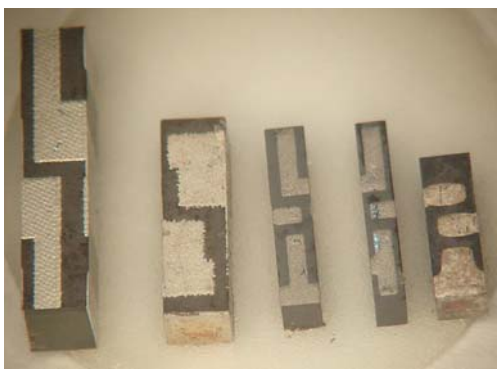

Fig. 6 Piezoelectric stators in various dimensions: length changing from 3.5 to 7.0 mm. A constant length to thickness ratio of 3.3 was maintained for all stators

Cases 5 and 6 are equivalent to Cases 3 and 4, respectively. The difference is channel 2 is excited and channel 1 was either leaved floating (Case 5) or shorted to ground (Case 6).

The effect of friction tip on operating resonance modes is lowering resonance and anti resonance frequencies of both first longitudinal and second bending modes. In addition, magnitudes of admittance values are decreasing slightly. To excite only first longitudinal mode Ch1 and Ch2 is shorted and connected to "HIGH" side of impedance analyzer and ground terminal is connected to "LOW" side of impedance analyzer (Case 1). Since the structure in this configuration is a resonator type multilayer actuator, only longitudinal mode is excited. The magnitude and phase of the pure first longitudinal mode are the thin solid lines in Fig. 9 (the curves are labeled as "L1_W/TIP").

When Ch1 terminal was connected to "HIGH" side and Ch2 terminal to "LOW" side of impedance analyzer (leaving the ground terminal floating) only second bending mode was excited (Case 2). The magnitude and phase of the pure second bending mode are the thick solid line in Fig. 9 (the curves are labeled as "B2_W/TIP").

When Ch1 is connected to "HIGH" side and GRN terminal to "LOW" side of the impedance analyzer while leaving the Ch2 floating (Case 3), the first longitudinal and the second bending modes are excited at the same time. Magnitude and phase curves in Fig. 9(a) and (b) are labeled as "L1_B2_W/TIP".

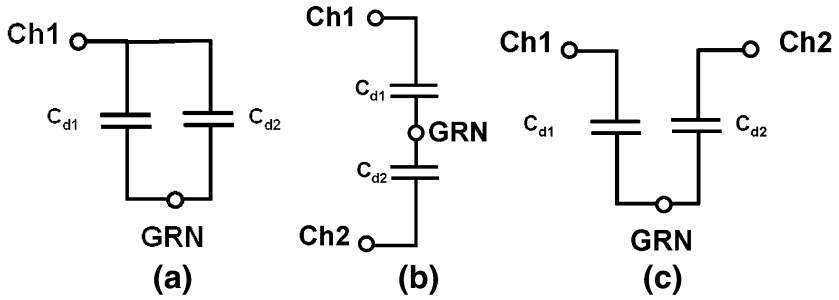

Fig. 7 DC capacitance values for different driving cases: (**a**) driving condition of case 1; DC capacitance values of channels 1 and 2 are connected in parallel. (**b**) Driving condition of case 2; DC capacitance of channels 1 and 2 are connected in series. (**c**) Regardless of the condition of unexcited channel, shorted to GRN or leaved open, the DC capacitance value is the capacitance of excited channel (Driving condition of case 3 and 4)

When Ch1 is connected to "HIGH" side and Ch2 and GRN terminals to "LOW" side of the impedance analyzer (Case 4), the first longitudinal and the second bending modes are excited at the same time. Magnitude and phase curves in Fig. 9(a) and (b) are labeled as "L1_B2_GRN_W/TIP".

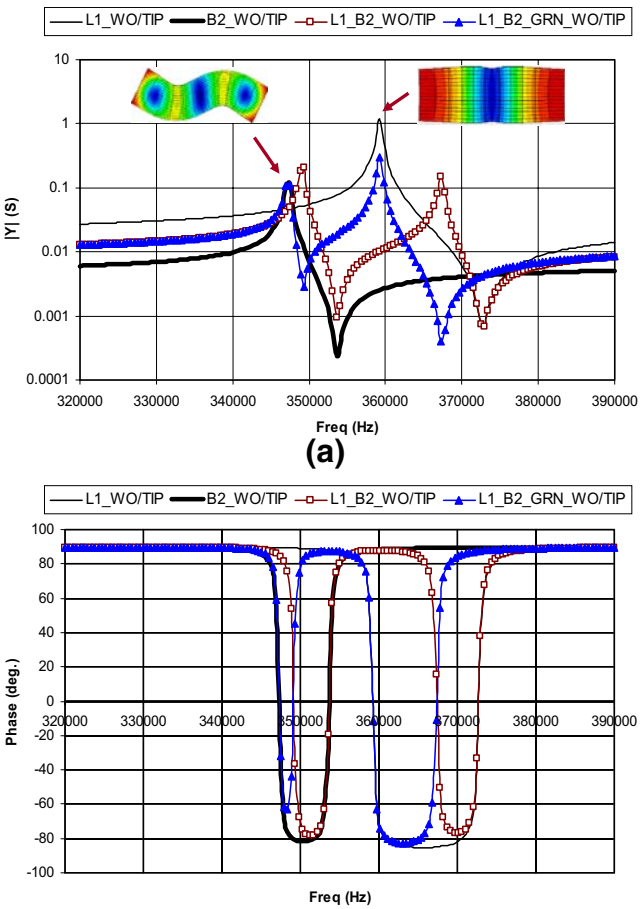

Fig. 8 Admittance magnitude (**a**) and phase (**b**) spectra for the excitation of first four cases; the curves labeled as "L1_WO/TIP", "B2_WO/TIP", "L1_B2_WO/TIP and "L1_B2_GRN_WO/TIP" are the admittance magnitude and phase plots of "Case1", "Case 2", "Case 3" and "Case 4" driving, respectively

Similar to before tip attachment case that magnitude and phase curves are plotted in Fig. 8(a) and (b); "Case 1" driving, first longitudinal mode anti resonance frequency and "Case 2" driving, second bending mode anti resonance frequency are equal to "Case 3" driving, anti resonance frequencies of first longitudinal and second bending modes. First longitudinal mode resonance frequency of "Case 1"

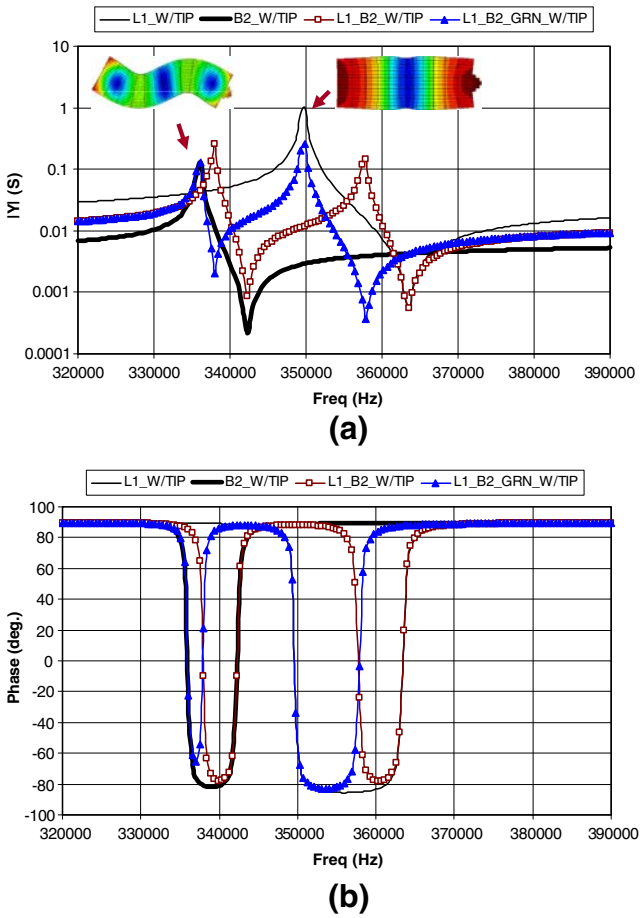

Fig. 9 Admittance magnitudes (**a**) and phase (**b**) spectra after friction element is attached on stator end. The curves labeled as "L1_W/TIP", "B2_W/TIP", "L1_B2_W/TIP and "L1_B2_GRN_W/TIP" are the admittance magnitude and phase plots of "Case1", "Case 2", "Case 3" and "Case 4" driving, respectively

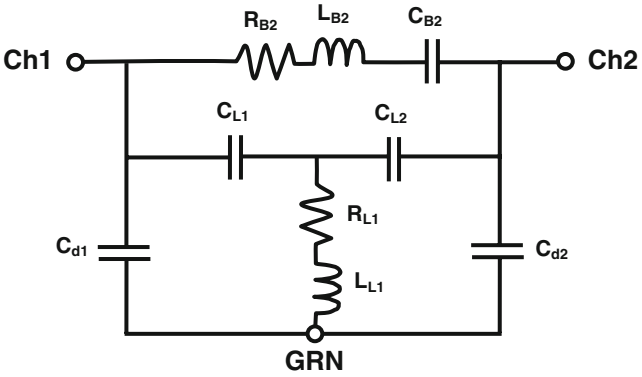

Fig. 10 Simplified electrical equivalent circuit of the free stator

driving and second bending mode resonance frequency of "Case 2" driving are equal to first longitudinal and second bending mode resonance frequency of "Case 4" driving.

From the six different driving cases of the free stator, an equivalent circuitry shown in Fig. 10 is introduced. We have already described how to find the parameters of DC capacitance values during different excitation case of stator. In the circuitry, C_{d1} and C_{d2} are the damping capacitance for channels 1 and 2, respectively.

The resonating circuit components can be obtained experimentally using admittance and phase data. L_{B2}, C_{B2} and R_{B2} are the equivalent inductor, equivalent capacitance and resonance resistance values that are related to second bending mode vibration. L_{L1} and R_{L1} are equivalent inductor and resonance resistance related to first longitudinal mode resonance of piezoelectric bar. The equivalent capacitance values at first longitudinal mode for channels 1 and 2 are modeled as C_{L1} and C_{L2}.

For example, for Case 1 driving, if Ch1 and Ch2 terminals are connected to "HIGH" side and GRN terminal

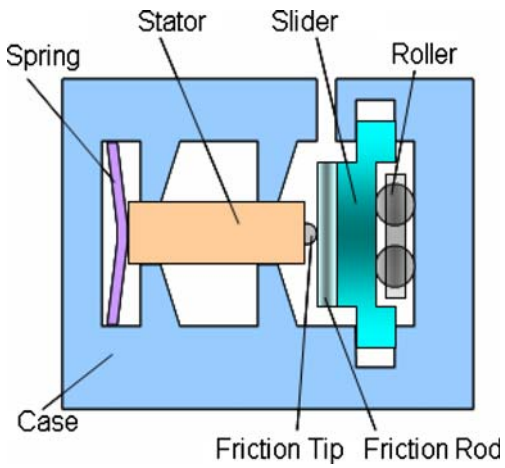

Fig. 11 Components of linear motor mechanism utilizing piezoelectric multilayered stator as the driver for linear positioning applications

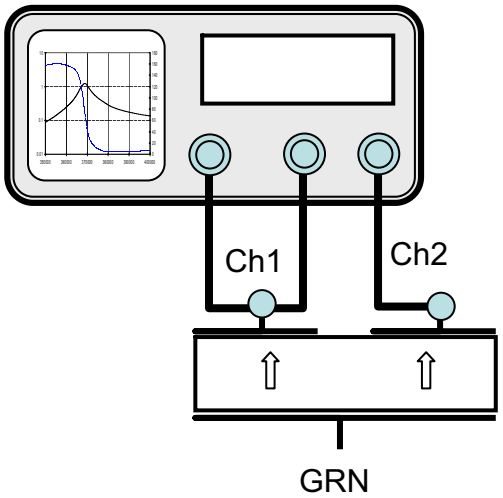

Fig. 12 Setup to measure gain and phase difference between driving and sensing channels

to "LOW" side of the impedance analyzer, equivalent resonance components of second bending mode (L_{B2}, C_{B2} and R_{B2}) will be cancel out and only first longitudinal resonance mode equivalent circuitry components will be

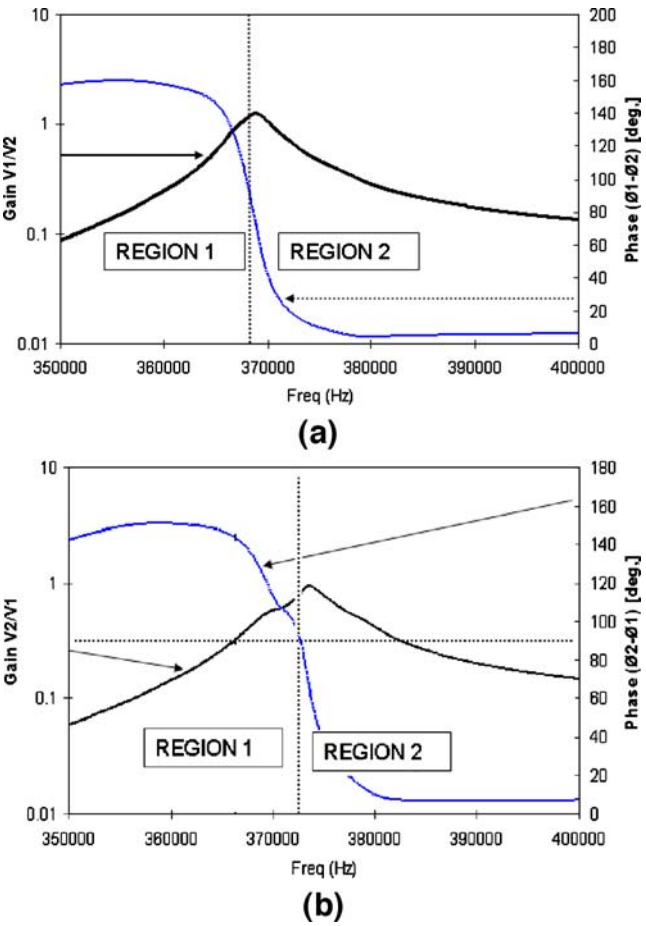

Fig. 13 Gain and the phase difference between Ch1 and Ch2. (**a**) When Ch1 is input and Ch2 is output (sensing), (**b**) When Ch2 is input and Ch1 is output

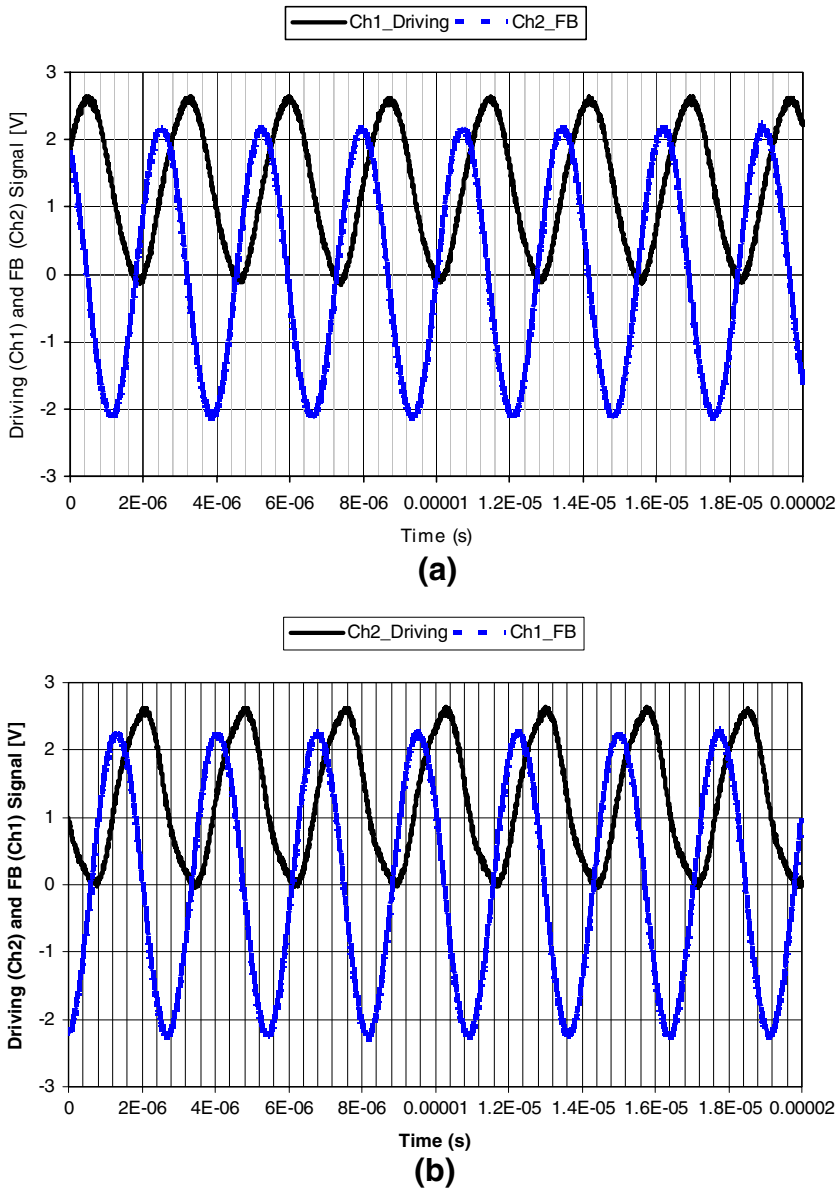

Fig. 14 Driving and sensing signals at the operating frequency of the motor showing the phase difference between Ch1 and Ch2: when Ch1 is input and Ch2 is output (**a**), when Ch2 is input and Ch1 is output (**b**)

excited. The resulting admittance spectrum will have only one peak which is pure first longitudinal mode (curves labeled as L1_W/TIP in Fig. 8 and L1_WO/TIP in Fig. 9).

For case 2 driving, only second bending mode resonance will be excited and equivalent inductor and resonance resistance (L_{L1} and R_{L1}) related to first longitudinal mode will be cancel out. Therefore, the resulting admittance spectrum will have only one peak which is second bending mode (curves labeled as B2_WO/TIP in Fig. 8 and B2_W/TIP in Fig. 9).

For case 3 driving, both first longitudinal and second bending mode resonance components will be excited and the resulting admittance spectrum will have two peaks which are first longitudinal mode and second bending modes. For Case 3 driving, admittance magnitude and phase curves in Figs. 8 and 9 are labeled as L1_B2_WO/TIP and L1_B2_W/TIP, respectively.

For case 4 driving, DC capacitance value, C_{d2} will be cancel out and as a result; both first longitudinal and second bending mode resonance components will be excited. For Case 4 driving, admittance magnitude and phase curves in Figs. 8 and 9 are labeled as L1_B2_GRN_WO/TIP and L1_B2_GRN_W/TIP, respectively.

The proposed equivalent circuitry can model after friction tip attachment on stator end. From the admittance magnitude and phase data before and after friction tip attachment (Figs. 8 and 9), we can see that the DC capacitance values of equivalent circuitry are not changing and frequency change could be related to mass thus indictor value increase due to friction tip attachment.

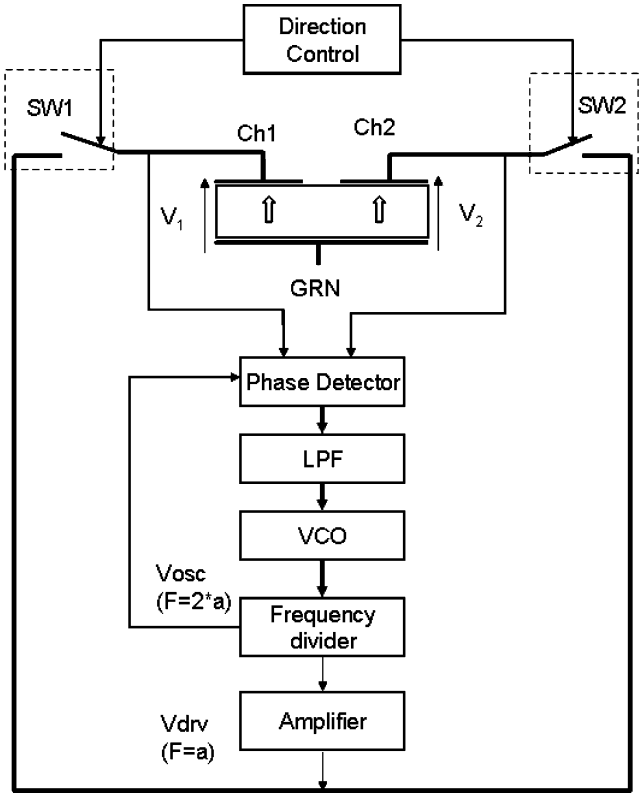

Fig. 15 Block diagram of driving circuitry showing the direction control and frequency tracking components

5 Stator in a linear motor structure

Simplified structure of a linear motor that comprises a stator composed of a piezoelectric vibrating unit with an attached frictional tip and a slider (see Fig. 11). The multi mode vibration generated by piezoelectric stator element is transferred to the slider through a guiding mechanism. The tip attached to the stator and the slider has a high friction low wear contact. A spring applies a pre stress to the stator to increase force transfer to the slider. A pair of roller creates a frictionless movement to the slider for an efficient transfer of vibration force from stator to the slider.

6 Operating frequency tracking method

When using piezoelectric motors for high volume applications, such as in lens moving mechanism for phone cameras, operating frequency can be different from sample to sample. In addition, at required operating temperature range of phone cameras (typically from −20 °C to +60 °C), an operating frequency drift can take place. In order for the driver circuitry handle these variations, a frequency tracking feature is needed. In this section, we will describe operating frequency tracking method of the piezoelectric motor proposed in this study.

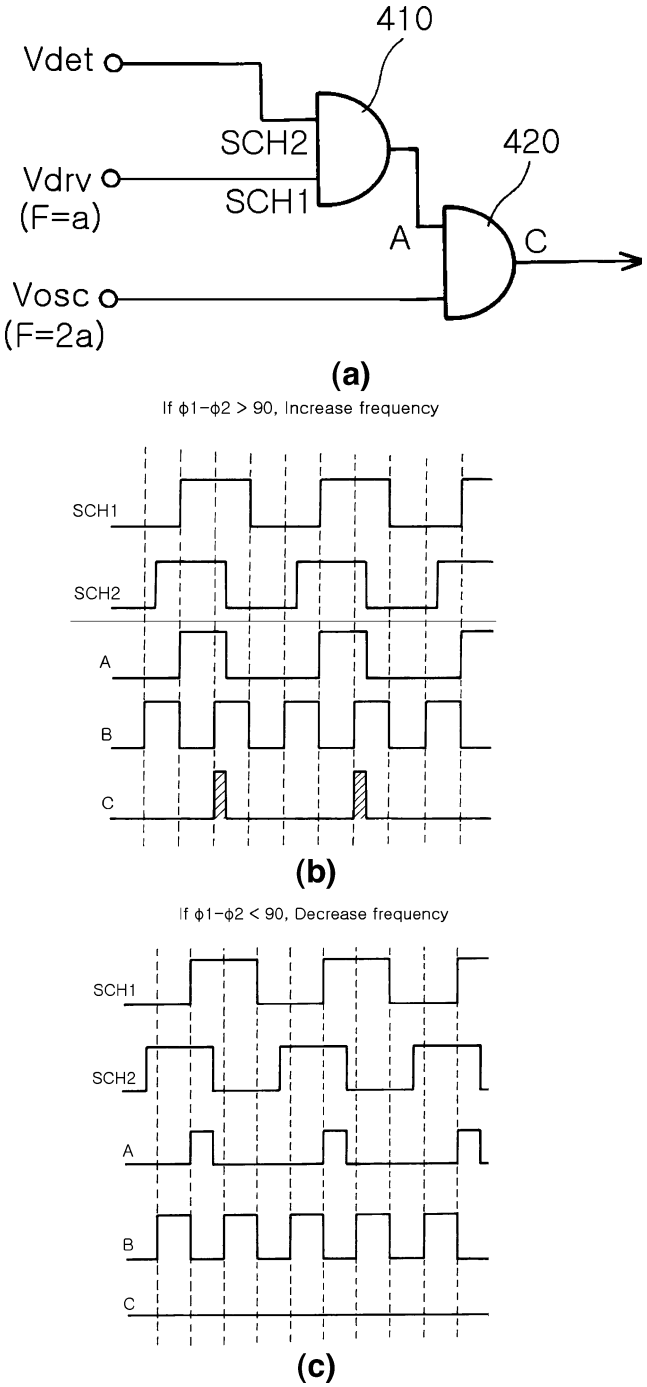

Fig. 16 (**a**) Phase detection logic, (**b**) logic waveform for the case that phase difference between Ch1 and Ch2 is greater than 90 degree so output control signal will force VCO to increase operating frequency, (**c**) logic waveform for the case that phase difference between Ch1 and Ch2 is less than 90 degree so output control signal will force vco to decrease operating frequency

We have already mentioned that the motor is operating with one channel driving. Since the stator is operating at resonance and due to piezoelectricity nature of it, a charge on unexcited channel is generated and this charge is creating an electric field between unexcited and ground electrodes. Depending on the vibration on stator, the

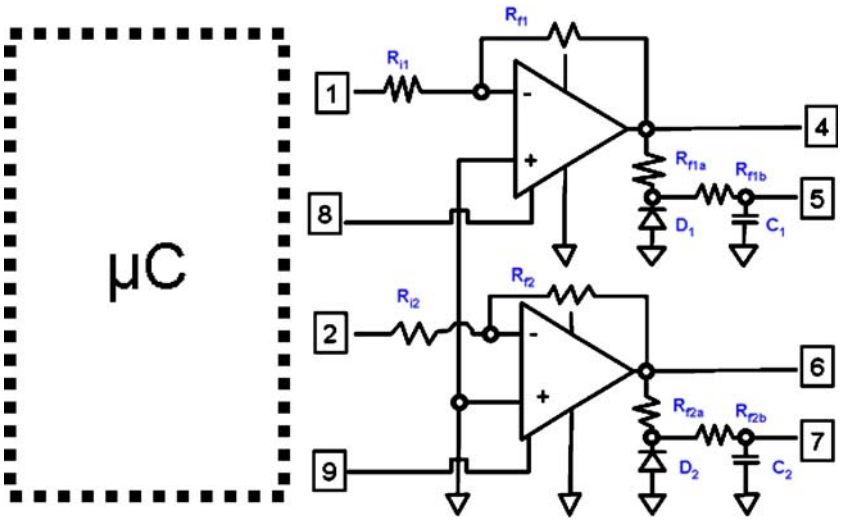

Fig. 17 Mixed mode excitation type piezoelectric motor driver with frequency tracking using a microcontroller and an OP-AMP pair

electrical signal generated on unexcited channel is used as a feedback. In fact, the stator element is acting as a piezoelectric transformer [13] that we have mentioned in section 4 during equivalent circuitry modeling.

Using FRA5095 impedance analyzer that the connection diagram is shown in Fig. 12, we have measured gain and phase difference between excited and unexcited channels. When Ch1 is excited and Ch2 is sensing the gain and phase difference between sensing and driving channels are shown in Fig. 13(a). As can be seen in the figure, at maximum gain point, the phase difference between channel 2 and channel 1 is 90 degree. When Ch2 is excited and Ch1 is sensing, a similar behavior was observed [Fig. 13(b)].

When the first channel, Ch1 is selected as the driving and Ch2 is sensing channel, the wave form of input and output signals are sown in Fig. 14(a). As can be seen from figure, the phase difference between input signal and output feedback signal is about 90 degree. When the second channel, Ch2 is selected as the driving and Ch1 is sensing channel, a similar behavior in term of phase difference was observed [Fig. 14(b)].

Figure 15 shows the block diagram of the driving circuitry of the single phase multi mode excitation type piezoelectric motor. If the efficient operating frequency of the motor is a frequency at which phase difference is 90 degree, the proposed circuitry will force the VCO to generate a frequency so that the motor operates at efficient point (for this particular example, the frequency is 365,000 Hz). It should be understood that there may be cases at which phase difference is other then 90°. It is also possible that a region of frequency at which the phase difference is in between two angles, such as 80 and 100°. Depending on pre-stress force on stator and mass of friction tip, set point of phase difference can be adjusted.

Even though most of the components in the driving circuitry such as phase detection, low pass filter (LPF), voltage controlled oscillator (VCO), frequency divider and direction control are handled by a microcontroller; a phase detection logic shown in Fig. 16(a) was used. Basically driving and detecting signals were first multiplied with logic AND gate and the resulting signal were again multiplied with the signal that VCO generates. Depending on the phase difference between driving and detecting signals, two types of control signals were generated [Fig. 16(b) and (c)]. If the driving frequency is in region 2 then the output control signal will be a positive value. If this value is higher than a set value (this value is upper boundary) then the frequency of VCO will be forced to decrease. If the driving frequency is in region 1, then the control signal will be zero (this value is lower boundary) than the frequency of VCO will be forced to increase.

By this way the driving frequency of the motor can be bounded into a narrow optimum operating frequency range. If the operating frequency of the motor is shifted due to environmental changes, such as temperature that resonance frequency dependency of piezoelectric resonator on temperature is well known, the circuitry will adjust the frequency region to an optimum operating region.

This developed driving method was realized using a microcontroller and a dual op-amp pair. In a simplified form, the circuitry is shown in Fig. 17. While an op-amp pair which is the amplifier part in the driving circuitry is boosting the current when driving both channels of the piezoelectric motor, a microcontroller handles all the other functions including direction control by using op-amps enable disable pins.

7 Conclusions

The motor presented in this study is a single phase-multi-mode-excitation type, which uses two orthogonal, first longitudinal and second bending, modes of a rectangular piezoelectric bar. The stator with optimum length to

thickness ratio of 3.3 and with unique electrode connectivity is highly mass producible in co-fired multilayer form at a size of as small as 3.5 mm. The low manufacturing cost of the stator make this motor to be suitable for high volume application such as for lens moving mechanism in phone cameras.

The electrical equivalent circuitry model can predict admittance characteristic of free stator very closely. We have also proposed an operating frequency tracking method for the linear motor. The proposed frequency tracking method was implemented using a microcontroller and a dual op-amp pairs.

References

1. K. Ragulsky, R. Bansevvicicus, R. Barauskas, G. Kulvietis, in *Vibromotors for Precision Microrobots*, ed. by Eugene Rivin (Hemisphere Publishing Corporation, 1988)
2. S. Ueha, Y. Tomikawa, *Ultrasonic Motors: Theory and Applications*. (Clarendon, Oxford UK, 1993)
3. T. Sashida, T. Kenjo, *An Introduction to Ultrasonic Motors*. (Clarendon, Oxford, UK, 1993)
4. K. Uchino, J.R. Giniewicz, *Micromechatronics*. (Marcel Dekker, New York, 2003)
5. K. Uchino, J.R. Giniewicz, *Piezoelectric actuators and ultrasonic motors*. (Kluwer, Boston, USA, 1997), pp. 265–273
6. A. Kumada, A piezoelectric ultrasonic motor. Jpn. J. Appl. Phys **24–2**, 739–741 (1985)
7. J. Tsujino, K. Nakai, K. Sako, N. Ikegami, K. Noda, R. Suzuki, Load characteristics and vibration loci at the driving surface of ultrasonic rotary motor using a longitudinal-torsional vibration converter. Jpn. J. Appl. Phys **37**, 2960–2965 (1998)Part 1, No.5B
8. M. Fleischer, D. Stain, H. Meixner, New type of piezoelectric ultrasonic motor. IEEE Trans. Ultrason. Ferroelect. Freq. Cont **36**, 614–619 (1989)
9. Y. Tomikawa, T. Takano, H. Umeda, Thin rotary and linear ultrasonic motors using double-mode piezoelectric vibrator of the first longitudinal and second bending modes. Jpn. J. Appl. Phys **33**, 3073–3078 (1992)
10. B. Koc, S. Cagatay, K. Uchino, A piezoelectric motor using two orthogonal bending modes of a hollow cylinder. IEEE Trans. Ultrason., Ferroelect., Freq. Contr **49**(4), 495–500 (2002)
11. V. Vishnevsky, et. al. USSR Patent No:851560, 1976
12. R. Bansiavichus, et. al. USSR Patent 693493, 1977
13. C.A. Rosen, in *Solid State Magnetic and Dielectric Devices*, 1st ed., ed. by H. W. Katz (Wiley, New York, 1959), Chap. 5, p. 170.
14. P. Gonnard, P.M. Schmitt, M. Brissaud, New equivalent lumped electrical circuit for piezoelectric transformers. Trans. Ultrason., Ferroelect., Freq. Contr. **53**(4), 802–809, 2006